LBL-27599

Lawrence Berkeley Laboratory
UNIVERSITY OF CALIFORNIA

Presented at the Workshop on Hadron Spectroscopy,
Vancouver, B.C., Canada, February 21, 1989

Low Energy $\bar{p}p$ Physics

C. Amsler and K. Crowe

February 1989

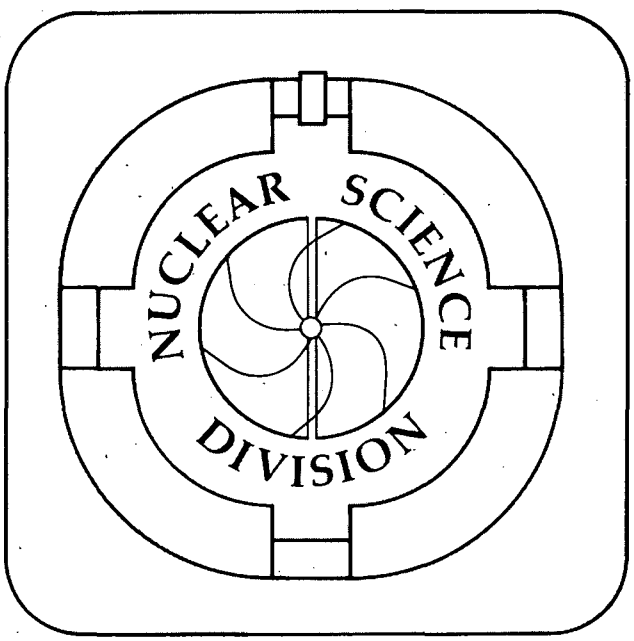

Prepared for the U.S. Department of Energy under Contract Number DE-AC03-76SF00098.

DISCLAIMER

LBL-27599

Low Energy $\bar{p}p$ Physics

C. Amsler
Physik-Institut, Universität Zürich
Schönberggasse 9, CH-8001 Zürich
Switzerland

K.M. Crowe
Physics Division
Lawrence Berkeley Laboratory
1 Cyclotron Road
Berkeley, California 94720
U.S.A.

Supported by the U.S. Department of Energy under Contract Number DE-AC03-76SF00098.

Low Energy $\bar{p}p$ Physics

C. Amsler
Physik-Institut, Universität Zürich, Schönberggasse 9, CH-8001 Zürich, Switzerland.
K.M. Crowe
Lawrence Berkeley Laboratory, Berkeley, CA94720, U.S.A..

1 Introduction:

A detailed investigation of proton-antiproton interactions at low energy has become feasible with the commissioning of the LEAR facility in 1983. We shall shortly review the status of $\bar{p}p$ annihilation at rest and the physics motivations for second generation experiments with the Crystal Barrel detector. This type of detector would be adequate for the study of both Kp and $\bar{p}p$ interactions on an extracted beam of the KAON Factory. We shall conclude with a few remarks on the physics opportunities with $\bar{p}$'s at the KAON Factory which, in *our* opinion, will not be covered by the present LEAR facility.

2 $\bar{p}p$ Annihilation at Low Energies:

The bulk of the available data has been collected with stopping antiprotons by bubble chamber experiments in the sixties with some 8 x 10^4 fully reconstructed pionic events and 2 x 10^4 kaonic events. Antiproton annihilation at rest in liquid hydrogen is dominated by capture from s orbitals (S wave annihilation) due to the quenching of the electromagnetic cascade. The contribution from p orbitals is only 8.6±1.1% [1]. The ASTERIX experiment at LEAR has increased the data sample by some two orders of magnitude for pionic channels using a gaseous hydrogen target at 1 atmosphere. In hydrogen gas the contribution of P wave annihilation increases to 50% [1,2]. In addition, a sample of nearly pure P waves was collected by triggering on the Balmer X-ray series (transitions to the 2p level) of the antiprotonic atom. The yield for the subsequent K_α X-ray transition to the 1s level being only 1%, the L-tagging leads to a sample of almost pure P wave. A background of about 10% (depending upon the annihilation channel) is due to bremsstrahlung from the emerging final state particles.

The capability to switch from S to P waves has led to the observation of interesting suppressions or enhancements in the production of final state mesons or resonances [1,2].

In spite of the now statistically impressive data sample, only 40% of the annihilation channels have been studied. This is due to the average π^0 multiplicity (1.5) in the final state. Channels with more than one π^0 cannot be reconstructed in bubble chambers. Even final states involving one η ($\rightarrow \gamma\gamma$) are hard to isolate since the missing η sits on a huge multi-π^0 background. The direct reconstruction of $\eta \rightarrow \pi^+\pi^-\pi^0$, although cleaner, suffers from combinatorial background with the other uncorrelated pions. The detection of final states involving η's is essential to the search for gluonic hadrons.

Data for $\bar{p}p$ annihilation in flight are rather scarce. The bulk stems from bubble chambers around 700 and 1200 MeV/c and there are nearly no data in flight below 700 MeV/c.

3 Physics Motivations:

3.1 Annihilation Dynamics:

Although this topic bears no relation to this workshop, we shall nevertheless mention it in view of the large number of theoretical papers recently published on this subject. The annihilation process was interpreted earlier in terms of resonance or baryon exchange in the t-channel. This type of approach, however, fails to reproduce the strong dependence on the initial $\bar{p}p$ angular momentum observed by ASTERIX, for instance the strong suppression of $\bar{p}p \rightarrow K\bar{K}$ when switching from S to P waves [1,2]. Baryon exchange implies a very short range (0.2 fm) for the annihilation force. Although the actual range is not known, it is generally believed to be at least of the order of the nucleon size. At this distance the p and $\bar{p}$ wavefunctions overlap so that the constituent quarks are expected to play an important role in the annihilation mechanism. For $\bar{p}p$ into two mesons, for example, the dominating contributions would then come from the annihilation of two quark pairs and the creation of a new pair (annihilation graph) or from the annihilation of one pair and the rearrangement of the other pairs (rearrangement graph). Each contribution to a given final state can be calculated and compared to the measured branching ratio. The relative rates of various channels can, for instance, be predicted from the quark line rule [3] (OZI rule) and the contribution from either graph obtained by comparison with data. On the experimental side, however, many two- and three-meson final states still need to be measured to allow a meaningful comparison with theory. Some of the branching ratios have been measured at the PS and at LEAR. Further data will be produced by the Crystal Barrel. It is not clear, however, whether a comprehensive picture will emerge before intensive $\bar{p}$ beams are available at the KAON Factory. Recent data from KEK show that these experiments can be performed even at rest on an intense external $\bar{p}$ beam.

3.2 Meson Spectroscopy:

We have heard at this workshop that glueballs and hybrid mesons are predicted in the 2 GeV mass range. Four quark $q^2\bar{q}^2$ states have been searched for at LEAR with negative success: narrow states are not observed in $\bar{p}p$ interactions but broad states might exist [4]. The strong P wave enhancement, discovered in low energy $\bar{p}p$ elastic scattering and in hyperon-antihyperon production close to threshold, has been explained in terms of P states close to the two-nucleon threshold [5]. This could be checked by searching for monochromatic low energy photons in $\bar{p}p \rightarrow \gamma X$ (where X decays into an exclusive final state and $E_\gamma \leq 100$ MeV).

Proton-antiproton annihilation is a prime but dirty source of gluons. Remember, however, that the $\eta(1430)$ (formerly called E/ι), a glueball candidate, was discovered twenty years ago in $\bar{p}p$ annihilation at rest. Figure 1 shows the production of a glueball and of a hybrid meson. Since the quantum numbers $J^{PC}(I^G)$ of a new state will have to be determined, a full kinematical reconstruction of the final state must be performed. At rest the angular distribution of the decay products is isotopic so that a 4π detector is required. Hopefully, states that cannot be built from a $q\bar{q}$ pair (CP exotics with $J^{PC} = 0^{--}$, 0^{+-}, 1^{-+}, 2^{+-}...) like the 1^{-+} $M(1406) \rightarrow \eta\pi$, recently reported by the GAMS Collaboration [6], will emerge. More likely, the spectroscopy of the 2 GeV mass range, where many $q\bar{q}$ states are still missing, will have to be unravelled first; before excess states that do not fit in the SU(3) classification are identified. Below 2 GeV the $\eta(1430)$, $f_0(1590)$ and $f_2(1720)$ are prime examples for such excess states.

Further clues for*(about)* gluonic content are obtained by studying the decay modes. While flavour is conserved in strong interaction decays of $q\bar{q}$ mesons (OZI rule), gluonic states couple more uniformly to s, d and u quarks. This requires a study of all decay modes, in particular into $\pi\pi$, $K\bar{K}$, $K^*\bar{K}$ and into the less conventional channels $\eta\eta$, $\eta\eta'$ and $\eta\pi$. The GAMS Collaboration now has evidence for several new states in the 2 GeV region, decaying into $\eta\eta$, $\eta\eta'$, $\omega\omega$ and $4\pi^0$. They need to be confirmed by another experiment, but they illustrate the discovery potential when switching to an entirely new experimental approach — the

detection of final states with several photons.

Since conventional mesons will also be produced, it is crucial to select the appropriate initial and final states. In liquid hydrogen at rest, only $^3S_1$ and $^1S_0$ ($\bar{p}p$) initial states contribute (apart from a small P wave contamination). A proper choice for the final state further reduces the number of contributing waves. For example, a state decaying into $\omega\pi^0$ ($\eta\pi^0$) would be investigated in $\bar{p}p \rightarrow \omega\pi^0\pi^0$ ($\eta\pi^0\pi^0$) for which only $^3S_1$ ($\bar{p}p$) and $^1S_0$ ($\bar{p}p$) contribute respectively. Furthermore, a final state involving two neutral pions is more suitable than $\pi^+\pi^-$ since the overwhelming ρ^0 does not couple to $\pi^0\pi^0$. The particular final state leading to the minimum combinatorial background should be selected. There are, for instance, four ways to combine four *(two)* charged pions in $\eta 2\pi^+ 2\pi^-$ to form the $\eta\pi^+\pi^-$ invariant mass; but only one in $\eta\pi^0\pi^0\pi^+\pi^-$. Thus final states with several neutrals are easier to reconstruct and analyse, provided that the detector has enough efficiency and energy resolution to disentangle the γ combinatorics.

4 The Crystal Barrel Experiment:

The goal is to search for states produced in $\bar{p}p$ annihilation, associated with the production of one or two pions:

$$\bar{p}p \rightarrow X^0\pi^0,\ X^{\pm}\pi^{\mp},\ X^0\pi^0\pi^0,\ X^0\pi^+\pi^-$$

$$X^0 \rightarrow \pi^0\pi^0,\ \eta\eta,\ \eta\eta',\ \eta\pi^0,\ \eta\pi\pi,\ \omega\omega,\ \omega\pi^0$$

$$\text{or } X^{\pm} \rightarrow \eta\pi^{\pm},\ \omega\pi^{\pm},\ \eta\pi^{\pm}\pi^0$$

The reconstruction of kaonic channels is also possible provided that the kaon momenta are not too large. States X below ~1.5 GeV can be studied at rest. The region up to ~2.2 GeV will be covered at the maximum possible LEAR momentum of 2 GeV/c.

Let me*(us)* illustrate, with a few examples, the typical questions that will be addressed:

- E(1420), a glueball candidate, was first observed in $\bar{p}p$ annihilation at rest but its spin-parity assignment (0^{-+}) has remained controversial since high energy experiments have identified a 1^{++} state at the same mass, the $f_1(1420)$. The 0^{-+} assignment has now been confirmed by the ASTERIX Collaboration [7] for the state observed in $\bar{p}p$ annihilation. E is presumably identical to $\eta(1430)$ (formerly ι) observed in radiative J/ψ decay. It decays into $K\bar{K}\pi$ via $a_0(980) \rightarrow K\bar{K}$, although $a_0 \rightarrow \eta\pi$ leading to $\iota \rightarrow \eta\pi\pi$ is not observed. One explanation for the puzzling absence of $\eta\pi\pi$ is that a_0 could be a $K\bar{K}$ molecule [8]. The $K\bar{K}$ threshold enhancement in $K\bar{K}\pi$ would then be due to phase space distortion by the nearby $K\bar{K}$ pole and not to the direct production of a_0. This will be verified by studying $\bar{p}p \rightarrow E\pi^+\pi^-$ ($E \rightarrow \pi^0\pi^0\eta$).
- The decay modes $E \rightarrow \rho\gamma,\ \omega\gamma,\ \phi\gamma$ will help to understand *(clarify)* the nature of E ($q\bar{q}$ or gluonic).
- The reported exotic $C(1480) \rightarrow \phi\pi$ from Serpukhov [9] will be searched for in $\bar{p}p \rightarrow \phi\pi^0\pi^0$. Preliminary data from the ASTERIX Collaboration for $\phi\pi^+\pi^-$ in gas [10] do not show evidence for this state (but on the other hand they do for the OZI suppressed $b_1(1235) \rightarrow \phi\pi$). A spin-parity analysis could not be performed due to limited statistics. The channel $\phi\pi^0\pi^0$ in liquid should be easier to analyse due to the restricted number of waves ($^3S_1$ ($\bar{p}p$) only) and the absence of ρ production.

4.1 The Crystal Barrel Detector:

The Crystal Barrel is a joint venture of the Universities of Hamburg, Karlsruhe, Mainz, Munich and Zurich, CRN-Strasbourg, CERN, LBL, RAL, UCLA and Queen Mary College.

The Crystal Barrel, Figure 2, detects charged and neutral particles over nearly 4π with a detection efficiency close to 100%. The antiprotons enter a solenoidal magnet (1.5 T) and interact in a liquid hydrogen target. Two cylindrical proportional wire chambers (PWC) provide the trigger for charged outgoing particles. The charged particle momentum is measured by a jet drift chamber (JDC) with 30 sectors, each with 23 signal wires. Charged π/K separation below 500 MeV/c is made by ionisation sampling. Photons are detected in a barrel shaped assembly of 1,380 CsI(Tl) crystals with photodiode readout. The liquid hydrogen target will be used at rest, where S wave annihilation dominates, and at 2 GeV/c. We will have the option of using a gaseous target to enhance P wave annihilation or the PWC's will even be replaced by an X-ray drift chamber to trigger on antiprotonic L X-rays and select P wave annihilation.

Table 1 compares the figures of merit for NaI, BGO and CsI. Caesium iodide is only weakly hygroscopic, hence does not need to be encapsulated, although it should be kept in a dry atmosphere (<30% humidity) to prevent a slow deterioration of the surface which has been treated (roughened) to yield a uniform light output along the crystal. The main disadvantage is the long decay time which limits the interaction rate at LEAR to a few 10^4 annihilations per second.

The 1,380 crystals are being manufactured by BDH-England. The delivery will be completed early in 1989. There are 13 different crystal shapes. The entrance face is roughly a square 3 x 3 cm^2. All crystals are oriented towards the interaction point and cover a solid angle of 98% of 4π. Each crystal, wrapped in teflon and aluminised mylar, is enclosed in a 100 μm thin *(thick)* titanium container for mechanical stability. The light (peaking at 550 nm) is collected at the rear end by a wavelength shifter. The reemitted light is detected by a photodiode glued on the edge of the wavelength shifter. The signal/noise ratio with one photodiode, using this method, is equivalent to the one obtained with four large photodiodes glued directly on the crystal, as shown in Figure 3. This technique thus allows substantial savings in the number of photodiodes and reduces the background in the photodiodes due to shower leakage (nuclear counter effect).

The supporting structure, which must sustain a weight of 4 tons, is an aluminium cylinder with a wall thickness of 10 mm.

The photodiode signal is amplified by a charge sensitive preamplifier mounted directly on each crystal, from which it is sent through a long twisted pair cable to a shaping amplifier. The 900 ns decay time of CsI determines the rise time of the preamplified pulse. The shaping amplifier differentiates the signal and generates a symmetric pulse, 6 μs long, which is fed into a charge integrating ADC. A fast converting 11-bit ADC, also used for triggering, covers the dynamical range up to 2 GeV. The range below 400 MeV is covered with improved resolution by a second 12-bit ADC. The electromagnetic showers initiated by high energy photons deposit energy in several adjacent crystals, so that the signals of 9 to 25 modules down to at least 1 MeV, must be added to obtain a good energy resolution. This sets rather stringent requirements on the noise level of the diode-preamplifier-shaper chain. A long integration time reduces the noise level but conflicts with the high rate expected at LEAR (~5 x 10^4 annihilations/s).

A preamplifier noise of σ = 200 keV has been achieved in the laboratory. The expected energy resolution for the sum of 25 crystal signals is:

$$\frac{\sigma}{E} = \frac{0.02}{\sqrt[4]{E(GeV)}}$$

Figure 4 shows the energy resolution calculated by EGS for 9 and 25 crystals. At low energy the sum of nine leads to a better resolution due to the contribution of preamplifier noise. The crystals will be calibrated with radioactive sources, cosmic rays and eventually with high energy photons from exclusive annihilation channels. The angular resolution depends upon the γ energy and is typically 20 mrad. Figure 5 shows the mass resolution for η and π and Figure 6 the momentum resolution.

A prototype of three sectors of the jet drift chamber has been built and tested in a 200 MeV/c pion beam at PSI/SIN. The sense wires of the central sector were read out on both ends by 100 MHz flash ADC's.

Figure 7 shows the distribution of the time difference between neighbouring signal wires. The alternating time shift of the signals is due to the 200 μm staggering of the sense wires, which is required to remove left-right ambiguities. These results indicate that the forecasted $\sigma = 100$ μm resolution in a CO_2/Isobutane gas mixture will be achieved. The coordinate along the wire is determined by charge division from signals from both ends of the wire. Figure 8 shows the distribution of the measured deviations from a straight line fit. A resolution of $\sigma = 5$ mm is achieved, in agreement with expectation. The full chamber, manufactured at LBL, has been delivered to CERN and has already received its first antiprotons. Figure 9 shows the expected momentum resolution for pions and kaons.

Since the annihilation rate at LEAR will be higher than the maximum possible data acquisition speed, a multilevel trigger is used. A scintillation counter signals an incoming $\bar{p}$ and provides the start time for the JDC. The two PWC's, which cover a solid angle of 99% of 4π, determine within 100 ns the charged multiplicity of the final state. Neutral kaons decaying into $\pi^+\pi^-$ between the chambers lead to an increase of multiplicity in the outer chamber. Since most K_S's decay before reaching the innermost chamber, the trigger efficiency on neutral kaons is about 10%. A hardwired processor determines within 10 μs the cluster multiplicity in the barrel and compares with a preset multiplicity. A 68020 processor then fetches the digitised energy deposits in the barrel and computes all combinations of two-photon invariant masses. This level requires 0.1 to 1 ms, depending upon the multiplicity, to provide a trigger on the number of π^0's and η's. A global event builder then also collects the digitised JDC information and transfers the data to tape via a μVAX 3600. The data acquisition rate is typically 50 events/s.

The reconstruction efficiency depends upon the $\bar{p}$ momentum and on the final state multiplicity since γ initiated showers and energy clusters from charged particles can overlap. This effect increases slightly at 2 GeV/c due to the forward Lorentz boost. For example, the reconstruction efficiency is 84% (64%) for $\pi^+\pi^-\eta$ ($\pi^+\pi^-\pi^0\pi^0$) at rest and 62% (24%) at 2 GeV/c. The effective γ detection probability is 94% (90%) and 87% (74%) respectively. Kinematical fitting is a powerful tool to separate the signal channel from background when all final state particles are detected. Except for channels with very low branching ratios ($<2 \times 10^{-3}$), we expect a background over signal ratio of less than a few %.

5 Proton-Antiproton Interaction in Flight:

The highest available beam momentum is 2 GeV/c ($\sqrt{s} = 2.43$ GeV) at the present LEAR facility (and the lowest 60 MeV/c). Since all users get the same beam momentum, experiments which require a variable antiproton momentum have faced a difficult scheduling problem as the machine then runs as a single user facility. This situation is unlikely to change in the future, since most time and beam consuming experiments (Crystal Barrel, CPLEAR, Obelix and the $\bar{p}$ mass experiments) require low beam momenta of 200 MeV/c or less.

5.1 Production of Mesons in the 2 GeV Range:

We have heard from N. Isgur that flux tube models and lattice gauge theories now locate glueballs in the 2–3 GeV mass range (apart from the scalar state at 1.5 GeV). These states, which could be produced in $\bar{p}p \rightarrow X\pi$ or $X\pi\pi$, would be inaccessible to LEAR. A whole spectrum of hybrid mesons is also predicted around 1.9 GeV [11]. These states decay into an S wave and a P wave meson, for example:

$$X \rightarrow b_1(1235)\pi\,, \quad b_1(1235) \rightarrow \omega\pi$$

or

$$X \rightarrow f_1(1285)\pi\,, \quad f_1(1285) \rightarrow a_0(980)\pi$$

These states will be looked for with the Crystal Barrel at LEAR and with 2 GeV/c $\bar{p}$. However, the uncertainty in the precise mass and the large width (>100 MeV), as well as the limited phase space, make it desireable to extend the $\bar{p}$ momenta up to at least 3 GeV/c. This type of experiment could be done on an extracted $\bar{p}$ beam at the KAON Factory with a flux of 10^6 $\bar{p}$/s. Above 2 GeV/c the forward Lorentz boost becomes significant, even for antiprotons, so that better forward coverage is required. Figure 10 shows the Crystal Barrel supplemented by a forward detector consisting of a dipole magnet, a particle identification system (TOF and Čerenkov) and a lead glass wall. Note that this device is similar to the facility proposed at this workshop for baryon and meson spectroscopy with K^- beams.

5.2 Meson formation in $\bar{p}p \rightarrow X \rightarrow M1M2$:

This type of experiment measures the excitation function as a function of $\bar{p}$ momentum in small momentum steps. For the formation of gluonic states one would select OZI forbidden processes like $\bar{p}p \rightarrow \phi\phi$ or dynamically suppressed processes like $\bar{p}p \rightarrow K_S K_S$ in order to reduce the background from the formation of conventional $q\bar{q}$ states. The channel $\phi\phi$ will be investigated at LEAR by JETSET. The $\xi(2230)$ reported by Mark III has been searched for at LEAR in $K_S K_S$ (and in K^+K^-) with negative results, although the sensitivity could still be improved by a large factor.

Two-body final states are also very restrictive on the quantum numbers of the s-channel resonance X, as shown in Table 2. One would measure the differential cross-section as a function of beam momentum, possibly with and without a polarised target, for reactions like $\bar{p}p \rightarrow \pi^0\pi^0$, $\pi^0\eta$, $\eta\eta$, $\eta\omega$, $\pi^0\omega$ etc.. Such reactions are suitable to locate broad resonances by means of a partial wave analysis and would shed light on the dynamics of $\bar{p}p$ annihilation. Thus far only few data exist below 2 GeV/c, mostly on $\pi\pi$ and $K\bar{K}$. The latter reaction shows a prominent backward peak in K^+K^- (corresponding to a forward K^+), the origin of which is not clear and a resonance behaviour of $K_S K_L$ was reported earlier. Additional information from $K_S K_S$, $K_S K_L$ and $\pi^0\pi^0$ below 1 GeV/c would be useful to understand the $\pi^+\pi^-$ and K^+K^- reactions.

In conclusion, while $\bar{p}p$ annihilation below $\sim$ 500 MeV/c would probably remain in the realm of LEAR, meson spectroscopy would benefit greatly from separated antiproton beams in the range 500 to 3,000 MeV/c at the KAON Factory.

References

[1] M. Doser et al., Nucl. Phys. A.

[2] M. Doser et al., Phys. Letters B.

[3] H. Genz, Phys. Rev. D28(1983)1094, D31(1985)1136.

[4] C. Amsler, Adv. Nucl. Phys. .

[5] I.S. Shapiro, Villars.

[6] F. Binon.

[7] ASTERIX Collaboration, Mainz, 1988.

[8] Weinstein and Isgur.

[9] S.I. Bityukov et al., Phys. Letters 188B(1987)383.

[10] M. Heel, Thessaloniki.

[11] N. Isgur.

Property	NaI(Tl)	BGO	CsI(Tl)	Units
λ_R	2.6	1.1	1.9	cm
ρ	3.7	7.1	4.4	g/cm^3
λ_{max}	420	480	550	nm
Y_{light}	1	0.1	1	
τ	230	300	900!	ns
\$	2	5–10	2	\$/cm^3

Table 1: A comparison of various scintillating crystals.

J^{PC}	I^G	$\pi^0\rho^0$	$\rho^0\rho^0$	$\rho^0\eta$	$\rho^0\omega$	ρ^0f	ωf	π^0f	$\pi^0\pi^0$	$\pi^0\omega$	$\pi^0\eta$	$\eta\eta$	$\eta\omega$
0^{-+}	0^+		x										
0^{++}	0^+		x						x			x	
0^{-+}	1^-				x			x					
0^{++}	1^-				x						x		
1^{+-}	0^-	x					x						x
1^{++}	0^+		x										
1^{--}	0^-	x					x						x
1^{+-}	1^+			x		x				x			
1^{++}	1^-				x			x					
1^{--}	1^+			x		x				x			
2^{-+}	0^+		x										
2^{--}	0^-	x					x						x
2^{++}	0^+		x						x			x	
2^{-+}	1^-				x			x					
2^{--}	1^+			x		x				x			
2^{++}	1^-				x			x			x		

Table 2: Quantum numbers (x) of two-meson states.

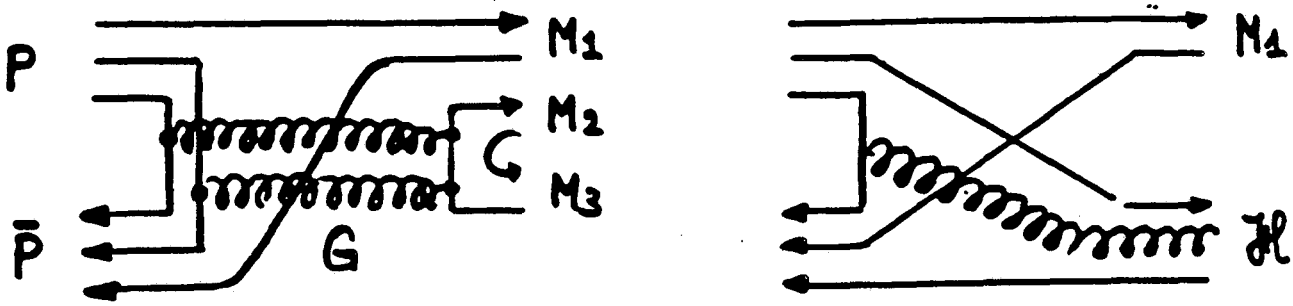

Figure 1: Production of a glueball (a) and of a hybrid (b) in $\bar{p}p$ annihilation.

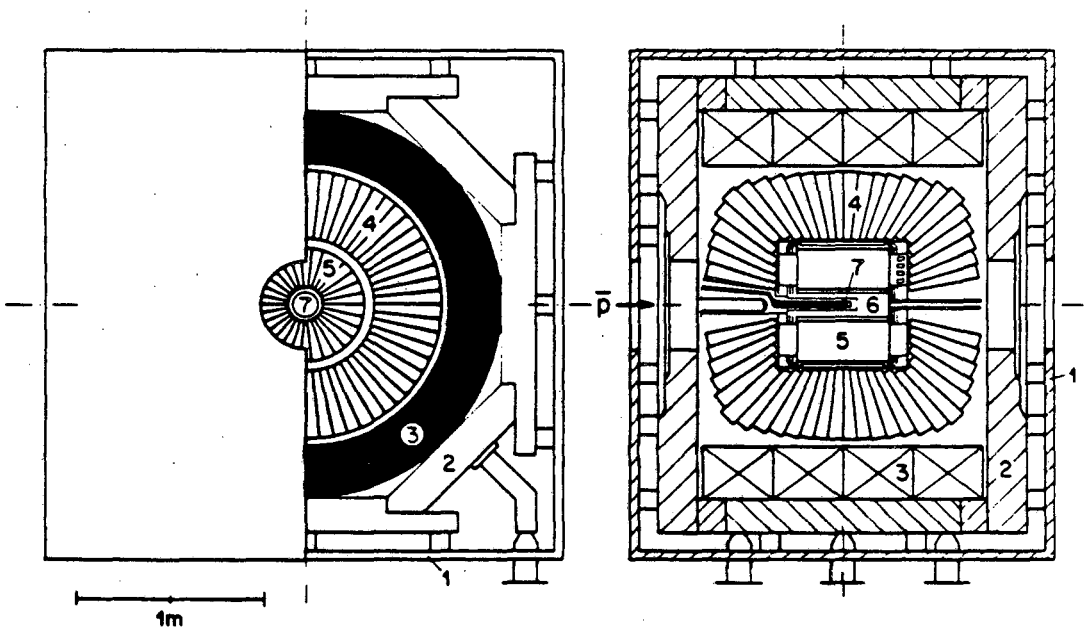

Figure 2: Crystal Barrel Detector. (1,2 – yoke, 3 – coil, 4 – CsI barrel, 5 – JDC, 6 – PWC, 7 – LH_2 target).

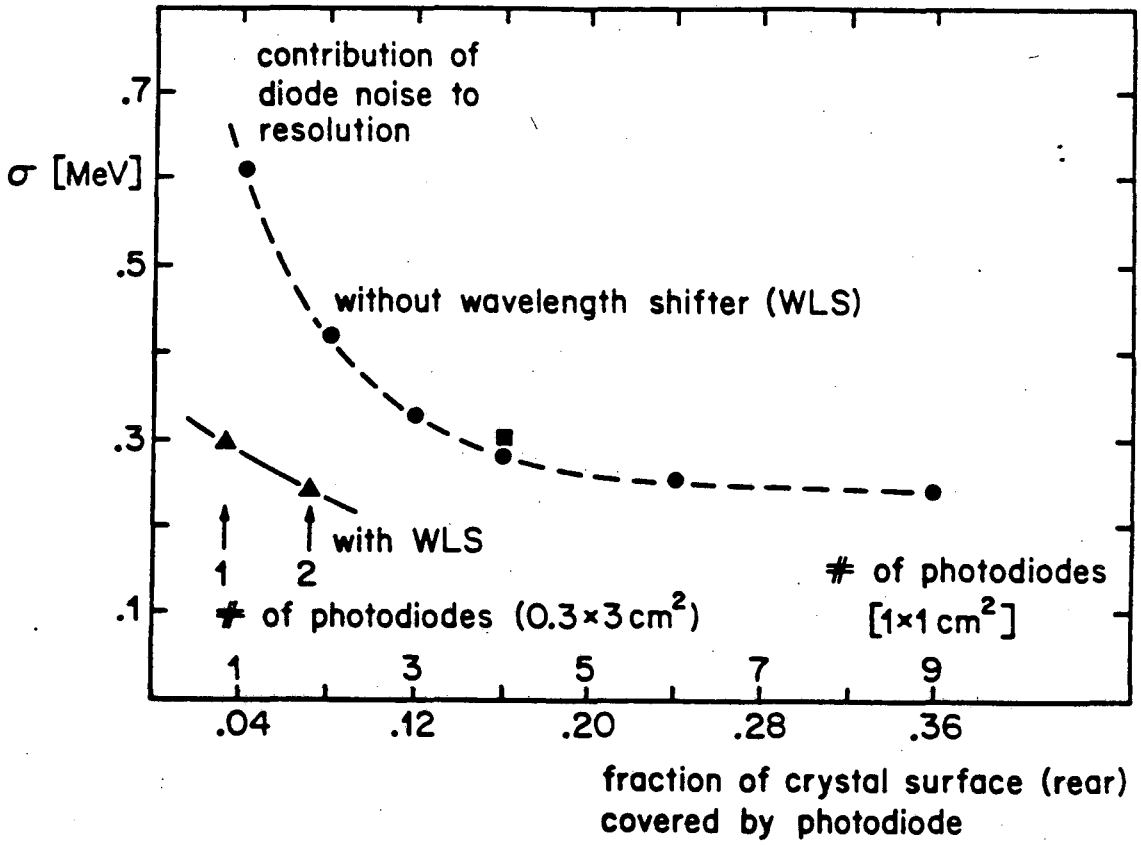

Figure 3: Performance of the wavelength shifter readout.

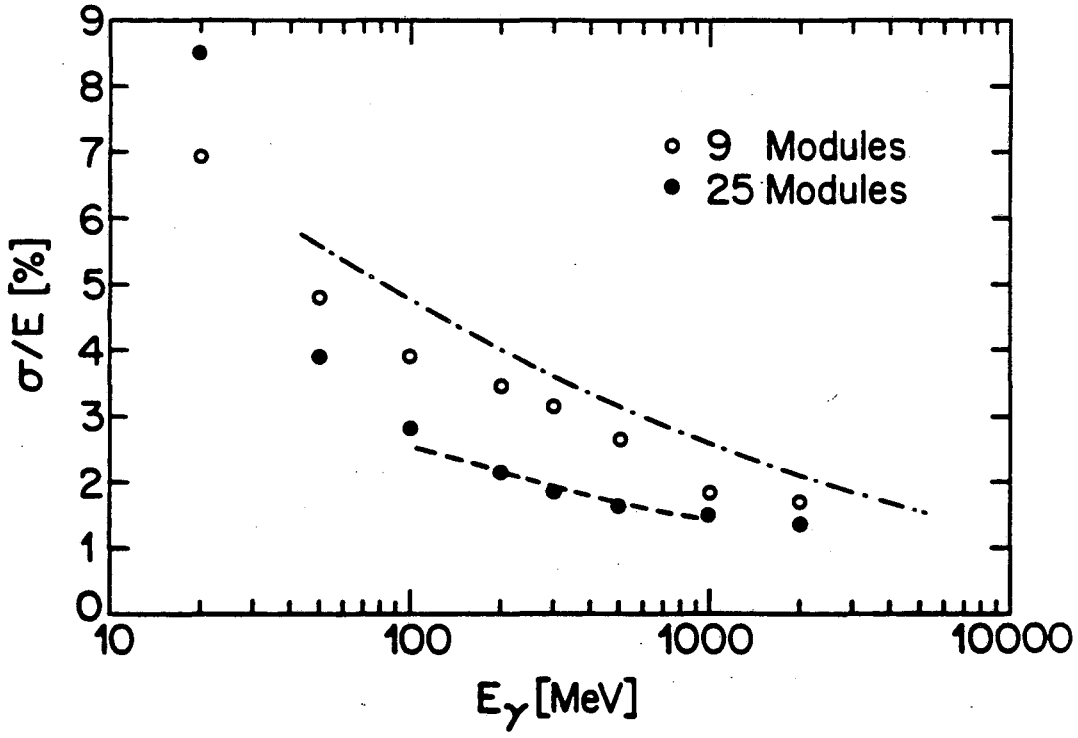

Figure 4: Energy resolution of the Crystal Barrel as a function of γ energy. Results are from EGS simulation with 0.3 MeV rms noise/module and 1.5 T magnetic field, for 25 modules added (•) and 9 modules added (o). Also shown are experimental results for the Stanford Crystal Ball (– · –) and the NaI Sector (– –).

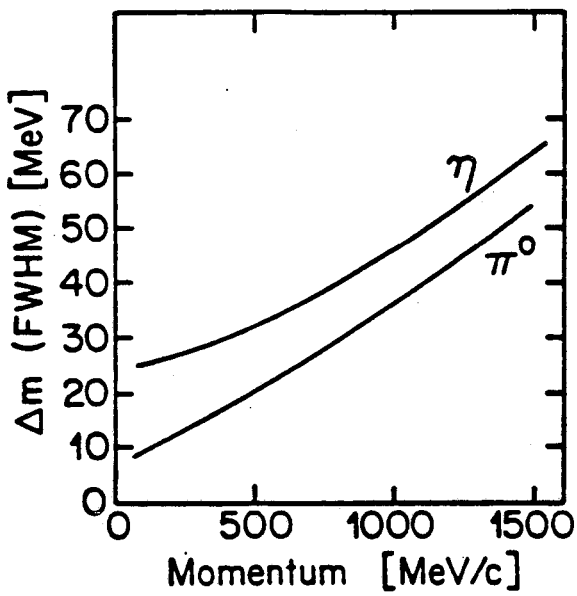

Figure 5: Mass resolution (FWHM) of the barrel.

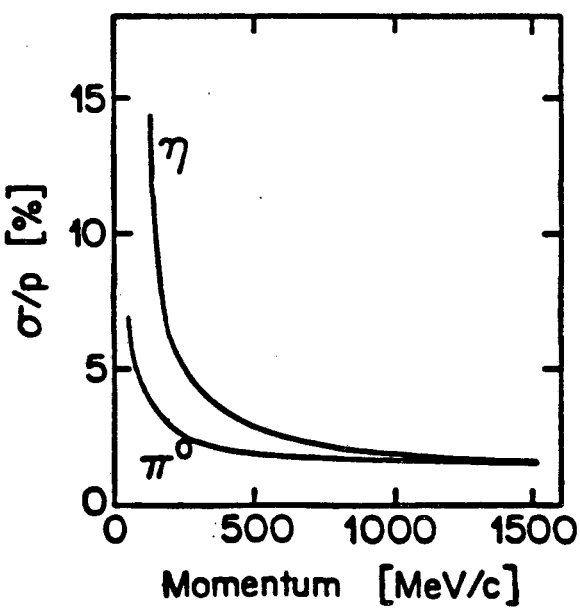

Figure 6: Momentum resolution (σ/p) of the barrel.

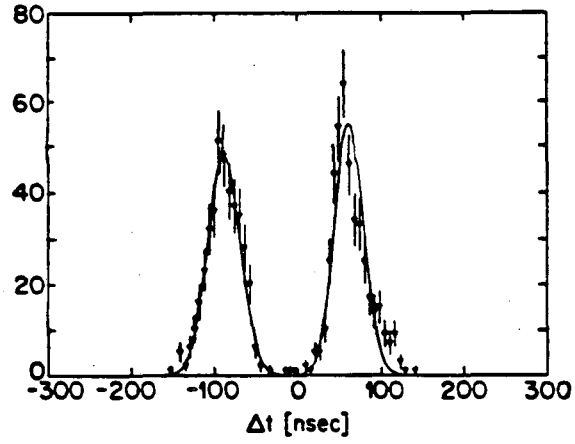

Figure 7: Distribution of the time difference between adjacent signal wires in the JDC. The time difference between the peak centroids corresponds to twice the staggering of 200 μm.

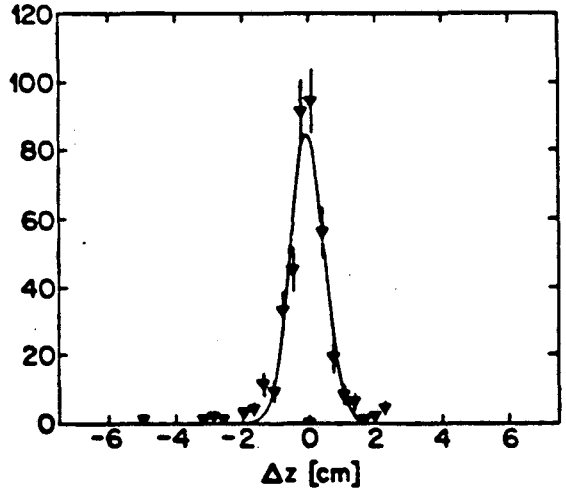

Figure 8: Position resolution by charge division on one JDC wire.

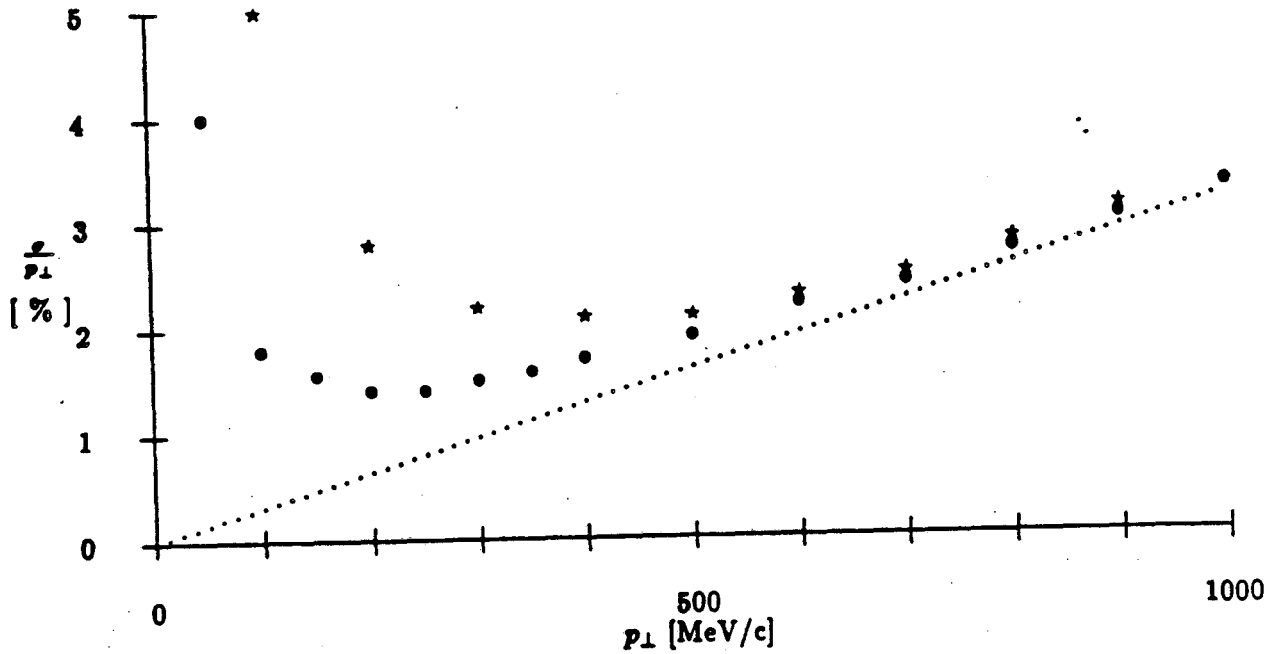

Figure 9: Chamber resolution as a function of transverse momentum, $p_\perp$. • is for pions and * is for kaons. The diagonal dashed line is the resolution limit only from measurement errors, assuming 23 points per track.

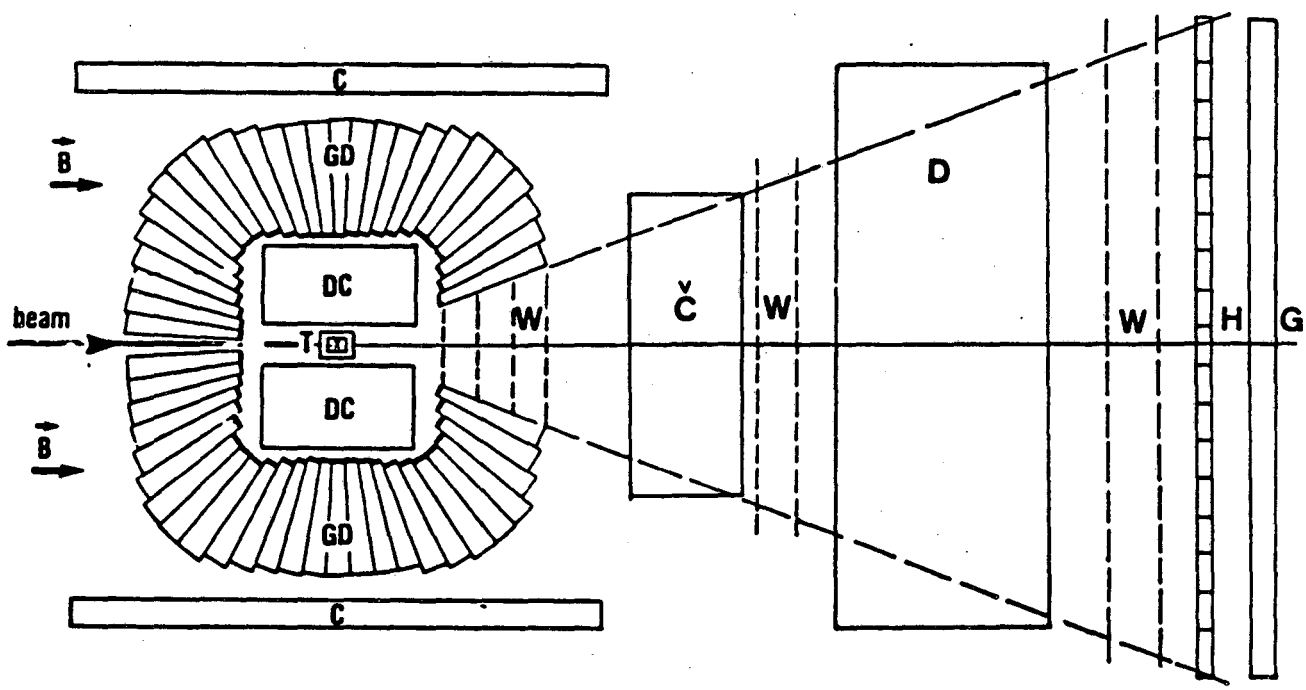

Figure 10: $\bar{p}p$ or K^-p facility using the Crystal Barrel. (C – solenoid, DC – drift chamber, GD – CsI barrel, T – LH_2 target, W – PWC, Č – Čerenkov, D – dipole magnet, H – hodoscope, G – lead glass hodoscope).

LAWRENCE BERKELEY LABORATORY
TECHNICAL INFORMATION DEPARTMENT
1 CYCLOTRON ROAD
BERKELEY, CALIFORNIA 94720